Optimum Design Parameters for a Spin-Stabilized Spacecraft Nutation Damper

GERALD J. CLOUTIER*
Hughes Aircraft Company, El Segundo, Calif.

Nomenclature

A = spacecraft moment of inertia about a transverse axis (not including damper mass)
C = spacecraft moment of inertia about the spin axis
T = kinetic energy
a = maximum amplitude of mass
c = damping constant
k = spring constant
m = mass
u, v = elastic displacements of the mass
Ω = nutation frequency
ζ = damping ratio
θ = nutation angle
τ = time constant
ω = angular velocity

Introduction

THE literature on nutation dampers for controlling the motion of spin-stabilized spacecraft contains several papers concerning rotor-mounted linear dampers whose motion is essentially in a plane normal to the spin axis.[1,2] This type of damper is shown conceptually in Fig. 1, but the damper could physically be one of many possible designs, such as a cantilever beam or pendulum damper.

References 1 and 2 do not optimize the damper performance (i.e., maximize the nutation decay rate), but merely perform parametric studies. In Ref. 3 it is shown that maximizing the nutation decay rate, with no constraints on the damper motion, leads to the conclusion that perfectly tuning the damper results in instantaneous reduction of the nutation angle to zero, a physical impossibility. Reference 3 attempts to get around this problem by including the transient motion of the damper in the solution.

An alternate procedure is suggested by the analysis of Ref. 4 in which a despun platform-mounted damper was optimized. In that reference, the technique used was to specify the maximum allowable amplitude of the damper as a constraint and then to maximize the nutation decay rate, thereby obtaining a reasonable solution. The same procedure is used in this Note.

Analysis

The method of analysis of the system used herein is the "energy-sink" method, in which the basic, unperturbed (by the damper, that is) motion of the spacecraft is assumed to drive the damper. The equations of motion of the damper are solved to determine the energy dissipation rate, which is then compared to the kinetic energy of the spacecraft at various nutation angles in order to estimate the rate at which the nutational motion decays.

Most of the relevant equations necessary for this analysis have been derived many times elsewhere and are summarized in what follows. First of all, the free motion of a stably nutating spacecraft is, in spacecraft fixed coordinates, is given by

$$\omega_x = (C/A)\omega_z\theta \cos\Omega t \tag{1}$$

$$\omega_y = (C/A)\omega_z\theta \sin\Omega t \tag{2}$$

$$\omega_z = \text{const} \tag{3}$$

$$\Omega = (C - A/A)\omega_z \tag{4}$$

[see Ref. 2, Eq. (11), with vehicle axisymmetric].

The rate at which energy dissipation in the spacecraft alters the nutation angle can be estimated by consideration of energy and momentum integrals of the equations of motion which results in

$$\dot\theta = [(C - A)/CA\Omega^2]\,[\dot T/\theta^2]\theta \tag{5}$$

for small θ [cf. Ref. 5, Eq. (6)] where, for a linear system, the rate of change of kinetic energy, $\dot T$, is proportional to θ^2, so that $(\dot T/\theta^2)$ is independent of θ. The solution to this equation is

$$\theta = \theta_0 e^{t/\tau} \tag{6}$$

where the "time constant," τ, has the value

$$\tau = CA\Omega^2/[(C - A)(\dot T/\theta^2)] \tag{7}$$

The energy dissipation rate brought about by a periodically oscillating mass which is being driven by the spacecraft's nutation is

$$\dot T = \zeta m\omega_n\Omega^2(u_m{}^2 + v_m{}^2) \tag{8}$$

where u_m and v_m are the amplitudes of the x and y motions of the mass. (It is assumed that there is no z motion.) Then, Eq. (7) becomes

$$\tau = -[CA/(C - A)]\,\theta^2/\zeta m\omega_n(u_m{}^2 + v_m{}^2) \tag{9}$$

The next step is to determine expressions for the amplitudes of damper motion. The linearized equations of motion of the damper mass in the x and y directions are

$$\ddot u + 2\zeta\omega_n\dot u + \omega_n{}^2u - 2\omega_z\dot v = -z_0(\omega_z\omega_x + \dot\omega_y) \tag{10}$$

$$\ddot v + 2\zeta\omega_n\dot v + \omega_n{}^2v + 2\omega_z\dot u = -z_0(\omega_z\omega_y - \dot\omega_x) \tag{11}$$

where

$$\omega_n{}^2 = (k/m) - \omega_z{}^2 \tag{12}$$

and where, in accordance with the energy sink assumptions, the amplitudes of ω_x and ω_y are considered to be essentially constant over several cycles of motion; i.e., the relatively slow change in θ is neglected in obtaining solutions for the damper displacements.

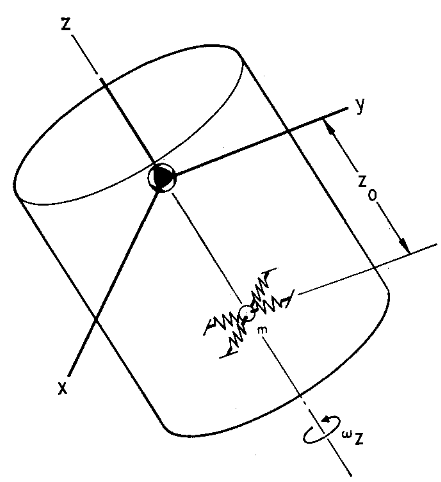

Fig. 1 Spinning spacecraft/nutation damper system.

Received September 24, 1971; revision received February 18, 1972.
Index category: Spacecraft Attitude Dynamics and Control.
* Staff Engineer, Space & Communications Group.

The solution to these equations will be examined for both one-degree-of-freedom (i.e., x motion only) and two-degree-of-freedom nutation dampers.

Thus the solution to Eq. (10), with $v = 0$ and ω_x and ω_y given by Eqs. (1) and (2), is

$$u_m{}^2 = \frac{[C/(C-A)]^4\theta^2 z_0{}^2}{[(\omega_n/\Omega)^2 - 1]^2 + (2\zeta\,\omega_n/\Omega)^2} \tag{13}$$

which, substituted into Eq. (9), yields

$$\tau_1 = -\left(\frac{C-A}{C}\right)^3 A\,\frac{[(\omega_n/\Omega)^2 - 1]^2 + (2\zeta(\omega_n/\Omega))^2}{\zeta m\omega_n z_0{}^2} \tag{14}$$

On the other hand, the solution to the two degree-of-freedom set, Eqs. (10) and (11), can be obtained by standard methods, and is

$$u_m{}^2 + v_m{}^2 = \frac{2[C/(C-A)]^4\theta^2 z_0{}^2}{[(\omega_n/\Omega)^2 - \{(C+A)/(C-A)\}]^2 + (2\zeta\,\omega_n/\Omega)^2} \tag{15}$$

which leads to

$$\tau_2 = -\left(\frac{C-A}{C}\right)^3 A\,\frac{[(\omega_n/\Omega)^2 - \{(C+A)/(C-A)\}]^2 + (2\zeta\,\omega_n/\Omega)^2}{2\zeta m\omega_n z_0{}^2} \tag{16}$$

Note that the time constant for this case is not merely ½ of that for the one degree-of-freedom case; the Coriolis coupling now enters into the expression.

Now the difficulty pointed out in Ref. 3 is evident. The minimum value of τ is obtained by tuning the damper (to eliminate the bracketed term in each expression) and by making $\zeta = 0$ which yields $\tau = 0$! This condition also results in $u_m = v_m = \infty$ and it is here that the energy sink characterization breaks down (as pointed out in Ref. 3). This solution implies that the unconstrained damper mass flies out to a very large amplitude, almost instantaneously absorbing all of the cross-spin kinetic energy of the spacecraft. Now, in accordance with the energy-sink assumptions, the wildly oscillating damper does not react back on spacecraft while the spacecraft, reduced to zero nutation, no longer forces the damper.

However, the motion of any actual damper will be limited by physical considerations. If this fact is used as a constraint on the allowable damper amplitude, a logical solution can be obtained. First, it will be assumed that there exists a maximum expected nutation angle θ_m to be designed for. Further, it is assumed that the damper will be most effective working at its maximum amplitude in this situation. Hence, set

$$u_m = v_m = a \tag{17}$$

for the case where $\theta = \theta_m$. In terms of nutation angle and maximum allowable damper amplitude a, the time constants are given [from Eq. (9)] by the following expressions:

One-degree-of-freedom system:

$$\tau_1 = -\frac{[CA/(C-A)]\theta_m{}^2}{ma^2\zeta\omega_n} \tag{18}$$

Two-degree-of-freedom system:

$$\tau_2 = -\frac{[CA/(C-A)]\theta_m{}^2}{2ma^2\zeta\omega_n} \tag{19}$$

Solving Eq. (13) for the damping ratio and substituting into Eq. (18) yields

$$\tau_1 = \frac{-2[CA/(C-A)]\theta_m{}^2}{ma^2\Omega\{[C/(C-A)]^4\,\theta_m{}^2 z_0{}^2/a^2 - [(\omega_n/\Omega)^2 - 1]^2\}^{1/2}} \tag{20}$$

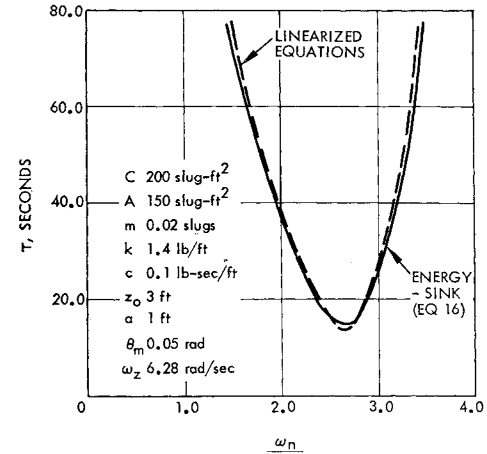

Fig. 2 Nutation decay time constant vs tuning.

Similarly, substituting Eq. (15) into (19) yields

$$\tau_2 = \frac{-\{CA/(C-A)\}\theta_m{}^2}{ma^2\Omega\left\{\left(\frac{C}{C-A}\right)^4 \frac{\theta_m{}^2 z_0{}^2}{a^2} - \left[\left(\frac{\omega_n}{\Omega}\right)^2 - \frac{C+A}{C-A}\right]^2\right\}^{1/2}} \tag{21}$$

By direct inspection of the quantities in braces in Eq. (20) and (21), it can be seen that τ_1 is optimized by setting

One-degree-of-freedom system:

$$(\omega_n/\Omega) = 1 \tag{22}$$

and τ_2 is optimized by setting

Two-degrees-of-freedom system:

$$(\omega_n/\Omega)^2 = (C+A)/(C-A) \tag{23}$$

The optimum parameters for the one-degree-of-freedom are thus

$$(\tau_1)_{\text{opt.}} = -2\theta_m A(C-A)/ma\Omega z_0 C \tag{24}$$

$$(\zeta_1)_{\text{opt.}} = -(1/2)[C/(C-A)]^2(\theta_m z_0/a) \tag{25}$$

and for the two-degrees-of-freedom are

$$(\tau_2)_{\text{opt.}} = -\theta_m A(C-A)/ma\Omega z_0 C \tag{26}$$

$$(\zeta_2)_{\text{opt.}} = (1/2)[C/(C-A)]^2[(C-A)/(C+A)]^{1/2}(\theta_m z_0/a) \tag{27}$$

Equations (22–27) thus give the damper parameters, ω_n and ζ, for the optimum time constant. To check the validity of these expressions, derived from energy sink considerations, computer runs were made using the complete, although linearized, equations of motion of a coupled spacecraft/two-degree-of-freedom damper system (such as those given in Ref. 6, specialized to substitute a single flexible mass).

Parametric studies of this sample case are summarized on Fig. 2, which also lists the particular spacecraft and damper parameters used. Here, the time constants obtained by using the linearized equations of motion and by using the energy-sink relation, Eq. (16), are plotted vs the damper's tuning. It can be seen that the energy-sink criterion for optimum tuning is justified for this example.

Conclusions

Modifying the energy-sink approach to nutation damper design by taking account of physical constraints on damper motion does indeed permit the derivation of simple relations for optimizing the damper parameters. The equations derived above are thus applicable to the preliminary design of a class of dampers used on the rotors of spin-stabilized spacecraft.

References

[1] Wadleigh, K. H. et al, "Spinning Vehicle Nutation Damper," *Journal of Spacecraft and Rockets*, Vol. 1, No. 6, Nov.–Dec. 1964, pp. 588–592.

[2] Alper, J. R., "Analysis of Pendulum Damper for Satellite Wobble Damping," *Journal of Spacecraft and Rockets*, Vol. 2, No. 1, Jan.–Feb. 1965, pp. 50–54.

[3] Austin, F. and Zetkov, G. A., "Zero Mass-Shift Passive Damper for the Reduction of Precession in a Rotating Space Vehicle," *Journal of the Astronautical Sciences*, Vol. XVI, No. 1, Jan.–Feb. 1969, pp. 1–7.

[4] Cloutier, G. J., "Nutation Damper Design Principles for Dual-Spin Spacecraft," *Journal of the Astronautical Sciences*, Vol. XVI, No. 2, March–April 1969, pp. 79–87.

[5] Thomson, W. T. and Reiter, G. S., "Attitude Drift of Space Vehicles," *Journal of the Astronautical Sciences*, Vol. VII, No. 2, Summer 1960, pp. 29–34.

[6] Meirovitch, L. and Nelson, H. D., "On the High-Spin Motion Satellite Containing Elastic Parts," *Journal of Spacecraft and Rockets*, Vol. 3, No. 11, Nov. 1966, pp. 1597–1602.

Motion of Bubbles in a Rotating Container

IVAN CATTON*
University of California, Los Angeles, Calif.
AND
S. H. SCHWARTZ†
West Virginia University, Morgantown, West Va.

Nomenclature

a = acceleration
A_B = cross-sectional area of bubble
C_D = coefficient of drag
D = bubble diameter
g = gravitational constant
g_e = gravitational constant on the Earth
F_D = drag force
m = mass of liquid displaced by bubble
m_e = inertial mass
Re = Reynolds number
v = bubble velocity
V_B = bubble volume
$\dot{x}$ = velocity component in x direction
$\dot{z}$ = velocity component in z direction
ν = kinematic viscosity
ρ_l = liquid density
ρ_v = vapor density
$\Delta\rho = (\rho_l - \rho_v)$
σ = surface tension
θ = angle
ω = angular rotation

Introduction

THE basic goal is to examine the effect of the Coriolis force on the motion of bubbles after reaching steady state in a rotating system. The motion of bubbles, without rotation, will be in the opposite direction of the gravity vector. However, acceleration induced by artificially rotating the tank or due to the rotation about its own axis as it orbits the Earth, will cause the bubbles to travel in a direction at some angle with respect to the gravity vector. This will increase the time it takes a bubble to rise to the surface which may affect the liquid level rise in a low-gravity venting condition. In addition, the lateral motion of the bubbles away from the heated tank walls into the center portion of a tank may play a role in reducing thermal stratification.

Received October 22, 1971; revision received January 19, 1972.
Index categories: Multiphase Flows; Hydrodynamics.

* Assistant Professor of Engineering and Applied Science. Member AIAA.
† Associate Professor of Engineering.

Basic Equations

In writing the equations of motion for a bubble in a rotating system, an effective force on the bubble due to Coriolis accelerations must be considered. This, when added to the usual buoyancy force results in a bubble trajectory which can be significantly different from the case without rotation. The motion of the bubble will be taken to be two dimensional in a plane perpendicular to the axis of rotation. The geometry, coordinate system, as well as a force balance are given in Fig. 1.

Using Newton's second law for motion of the bubble results in the following equations for the x and z directions:

$$m\ddot{z} = (\rho_l - \rho_v)V_B[g_z + \omega^2(R - z)] - \tfrac{1}{2}C_D\rho_l A_B\dot{z}(\dot{z}^2 + \dot{x}^2)^{1/2} - 2m_e\omega\dot{x} \quad (1)$$

$$m\ddot{x} = (\rho_l - \rho_v)V_B[g_x + \omega^2 x] - \tfrac{1}{2}C_D\rho_l A_B\dot{x}(\dot{z}^2 + \dot{x}^2)^{1/2} + 2m_e\omega\dot{z} \quad (2)$$

For a given bubble, an expression for C_D is needed. A plot of C_D as a function of Reynolds number is given in Fig. 2 and it can be seen that C_D is not a single valued function. For a first approximation, the curve is broken into three distinct regions termed the Stokes flow regime, the transition regime and the spherical-cap regime. The transition regime describes the ellipsoidal bubble region falling between the spherical bubble domain and the spherical cap domain as described by Haberman and Morton.[1]

With this approach, it is possible to approximate the critical Reynolds numbers Re_t and Re_s where a bubble enters the transition or spherical-cap regimes. This is done by finding the intersection of the portion of the curve in the transition

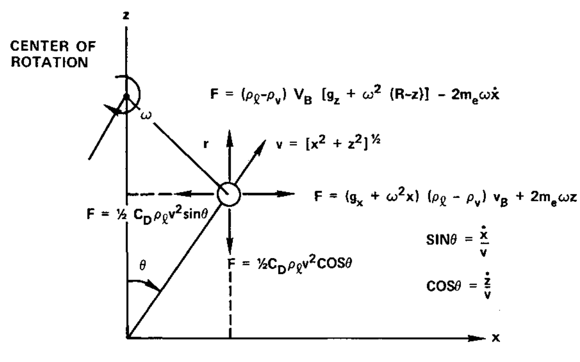

Fig. 1 Geometry, coordinate system and force balance on the bubble.

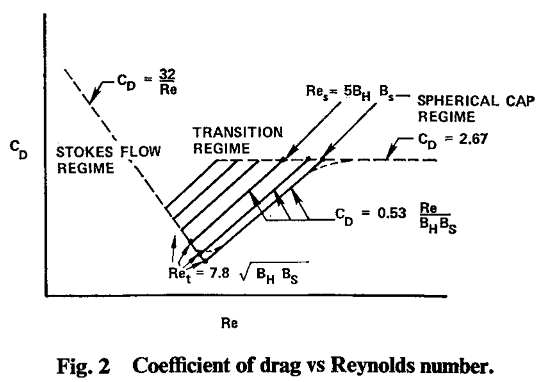

Fig. 2 Coefficient of drag vs Reynolds number.